

## TRANSFORMATIONAL PHENOMENON IN THE FIELD OF TAYLOR-COUETTE FLOW

Circular Couette flow or Taylor-Couette flow<sup>1,2</sup> is a classical problem of hydrodynamic stability; it is an important paradigm for determining the dynamics of sheared flows. Donnelly<sup>3</sup> and Simon and Donnelly<sup>4</sup> utilized the torque produced in a cylinder during viscous flow motions to measure the circular Couette flow at the critical point between stable and unstable flows. For inner and outer cylinders with the same rotational speed and direction, Taylor<sup>2</sup> demonstrated experimentally that when the rotational speed increases gradually to a speed exceeding critical speed, the flow still retains its one-dimensional flow state. In other words, the rotating outer cylinder is inhibited to maintain the stable state. Coles,<sup>5</sup> Schwarz et al.,<sup>6</sup> and Nissan et al.<sup>7</sup> obtained the same experimental results as Taylor did. More cases of time-modulated Taylor-Couette problems where the inner cylinder moves periodically in the axial direction were introduced and studied by Marques and Lopez.<sup>8,9</sup> Moreover, Walsh and Donnelly<sup>10</sup> demonstrated that when the rotational speed of the inner cylinder is fixed and the outer cylinder is under a cyclical motion, the flow is stabilized. Gollub and Swinney<sup>11</sup> and Walden and Donnelly<sup>12</sup> used laser Doppler anemometers (LDAs) to investigate the Taylor-Couette flow. The LDA is used to measure the radial temperature of flow measurement points. Through power spectrum analysis, the time domain is transformed into a frequency domain. The advantage of power spectrum analysis is that different characteristics of a spectrum represent different flow state. When the flow is periodic, a peak of a certain size forms on the spectrum of relative and harmonic frequencies. When the flow is transformed into a quasi-periodic flow, a frequency appears that is not associated with the original frequency. Power spectrum analysis is an efficient approach for studying the transformation between quasi-periodic and chaotic flows. For the modulated function, this study primarily focuses on the influence of modulated amplitudes and frequencies on the flow stability between cylinders. Donnelly<sup>13</sup> analyzed experimentally modulated flow stability. When the outer cylinder stays static and the inner cylinder rotates periodically, parameters such as the interval, rotational frequency, and modulated amplitude of the two cylinders can be changed to determine how the circular Couette flow is affected by modulated rotation. Hall<sup>14</sup> utilized linear theory to determine low and high frequencies and used nonlinear theory to analyze the flow under a high frequency. Carmi and Tustaniwskyj<sup>15</sup> examined modulated stability under a limited gap and the influence of axis symmetry and asymmetry on modulated flow. In a former study, the critical Reynolds number has an increased unstable offset at low frequencies. Youd et al.,<sup>16</sup> who analyzed a zero-equivalent modulated flow around concentric cylinders with a radius ratio of  $\eta = 0.75$ , identified the axis symmetry of the Taylor vortex. Walsh et al.<sup>17</sup> experimentally

measured the critical Reynolds number for a concentric cylinder with different radius ratios. The obtained Reynolds number was multiplied by a factor, and the resulting value was roughly the same as that calculated by Carmi and Tustaniwskyj.<sup>15</sup> Ganske et al.<sup>18</sup> utilized a scenario with a static outer cylinder and modulated vortex flow in the inner cylinder to investigate the influence of different amplitudes on stability. They demonstrated that the modulated effect causes the flow to become increasingly unstable and that amplitude has a significantly more important effect on flow stability than frequency.

This experiment uses flow observations and optical measurements to determine the flow stability and to determine the critical Reynolds numbers under different modulated amplitudes  $\varepsilon$  and modulated frequencies  $\omega'$ . The inner cylinder rotates at  $\overline{\Omega}(1 + \varepsilon \cos \omega't)$ , where  $\overline{\Omega}$  is the average angular velocity, the outer cylinder remains stationary, and the radius ratio is  $\eta = 0.4833$ ; the aspect ratio, defined as  $h = H/d$  where  $H$  is the cylinder length and  $d = R_2 - R_1$ , is  $h \leq 24$ . The Reynolds number  $Re = R_1 \overline{\Omega} d / \nu$ , where  $R_1$  is the radius of the inner cylinder represents the ratio of inertia to viscous force. The definition of stable state in this experiment is as follows: in each modulated cycle, if the disturbance decays immediately, it is determined to be stable. If the disturbance appears in any modulated cycle, the flow is unstable. If the disturbance only appears sometimes, the flow has transient stability.

### EXPERIMENT

Flow observations and optical measurements were utilized to determine when instability will occur. First, tiny particles (150–250  $\mu\text{m}$ ) of an aluminum slice or powder were added to the fluid. The aluminum powder density was roughly 0.2 g/L of fluid and used to increase the data rate and information availability. Figure 1 presents experimental equipment, including (1) the nonoptics area, which includes the flow observation area, transmission device, and control and information retrieval device; and (2) the optical area, which has a helium–neon laser tube, photoelectric receiver, LDA device, and oscillograph. A personal computer (PC) and PC-LabCard (PCL818, PCL816/814B, PCL889) were used to control and retrieve data. The control interface panel can output the predicted voltage value (corresponding rotational speed set in the experiment) and further control motor rotational speed. Table 1 lists experimental conditions for nonmodulated and modulated flows.

### Flow Observation Method

The moving orbit of particles determines the critical value of flow stability. This method can also observe the transformation process of unstable flows. The geometric structure of the observation area—which is chosen for convenience when observing the flow—includes an acrylic

W.M. Yang is an associate professor and H.C. Lin (herojake.lin@gmail.com) is a doctoral candidate with the Department of Mechanical Engineering, National Chiao Tung University, Taiwan, Republic of China.

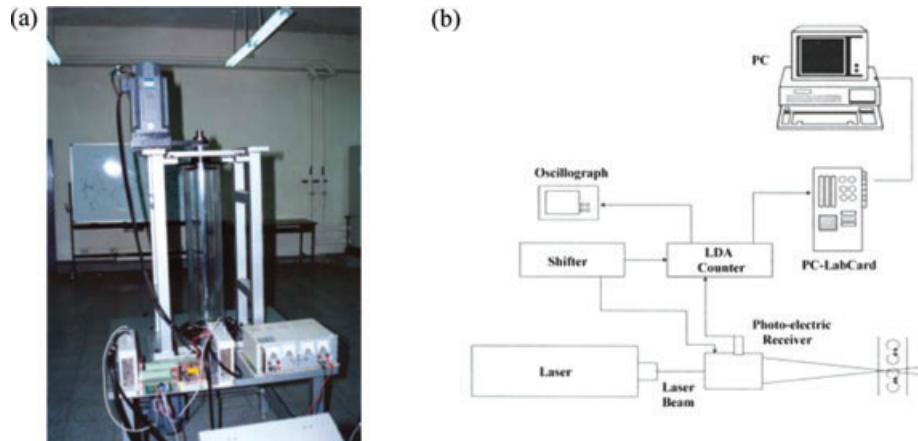


Fig. 1: Experiment setup for the Taylor-Couette apparatus with visualization techniques, (b) graph of the optics area

Table I—Experimental conditions for Couette flow

	NONMODULATED EFFECT	MODULATED EFFECT
Working fluid	Silicon oil (350p), SAE-10, SAE-20, SAE-30	Silicon oil (350p), SAE-20, SAE-30
Radius ratio	$\eta = 0.4833$	$\eta = 0.4833$
Aspect ratio	$h \cong 24$	$h \leq 24$
Upper and Lower B.C.	Fixed boundaries	Fixed boundaries
Rotational speed setting	Steady rotational output of 100–300 RPM	Periodic output of 0–600 RPM
Modulated amplitude range	None	$\varepsilon \leq 1$
Modulated frequency range	None	$\omega' = 0.0 = 0.006 \sim 18(1/s)$

rod 800-mm long with an inner diameter of 120 mm and wall thickness of 5 mm; this is used as the outer rod. The diameter of the inner steel rod is 58 mm. The distance between the inner and outer rod is  $d = 31$  mm. The ratio between the inner and outer rod is  $\eta = 0.4833$ . The inner rod has two dish-shaped devices that adjust the length of the flow area. The longest length is  $H = 750$  mm, which equals the largest aspect ratio of  $h \cong 24$ .

### Optical Measurement Method

As the  $Re$  increases, the flow is transformed from a one-dimensional Couette flow to a two-dimensional Taylor vortex flow. Therefore, the transformation process causes a change in particle density distribution. As density changes, the light scattered by particles in the flow also changes. Voltage measured by an oscillograph also changes. The measured voltage of the flow before and after it becomes unstable obviously changes as well. This characteristic is employed to determine flow stability. The laser light is split into two bunches of light via the spectroscop and intersect in the fluid measurement area. The photoelectric receiver receives the light scattered by tiny particles in the fluid and transforms it into photo voltage. Figure 2a shows the relationship between photo voltage and Reynolds number under the nonmodulated effect. As the Reynolds number increases, the photo voltage drops suddenly from  $V_1$  to  $V_2$ . Figure 2b presents the change in photo voltage under the

modulated effect. In this figure, the relatively low and flat curve is the photo voltage of a one-dimensional periodic Couette flow. When  $Re$  increases until the flow become unstable, the photo voltage of a two-dimensional periodic Taylor vortex flow is the curve with relatively high periodic behavior.

In the experiment, the outer cylinder is stationary and the inner cylinder rotates with the nonzero mean modulated angular speed  $\Omega = \bar{\Omega}(1 + \varepsilon \cos \omega' t)$ . The Reynolds number  $Re_0$  (the subscript 0 is defined as the nonmodulated critical state) for the unstable state before implementation of the modulation effect must be calculated first. Therefore, the outer cylinder must be stopped first. The low rotational speed of the inner cylinder is increased to a high rotational speed. The LDA is utilized to measure the axial speed to determine the critical Reynolds number  $Re_0$  when the Couette flow transforms into a Taylor vortex flow. When a modulated rotation is added and the flow becomes unstable, the speed along the axis is a function of time. At that moment, the LDA measures the relationship between speed along the axis and time at the measurement point. After the axis speed of the Taylor vortex flow is measured, the data obtained from the fast Fourier transform (FFT) are used for spectrum analysis of the power spectrum. This can further elucidate the frequency of a periodic flow and the change in frequency during transformation of the flow attitude.

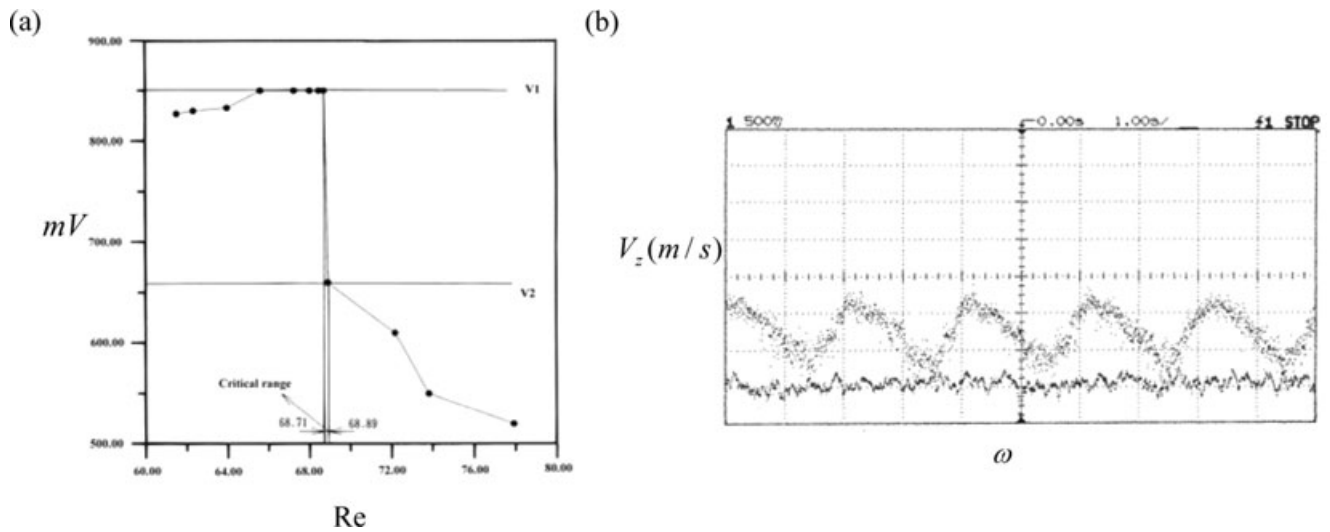


Fig. 2: Principle of the optical measurement method used to determine flow stability by photo voltage: (a) nonmodulated and (b) modulated frequency  $\omega' = 3.14$  (1/s)

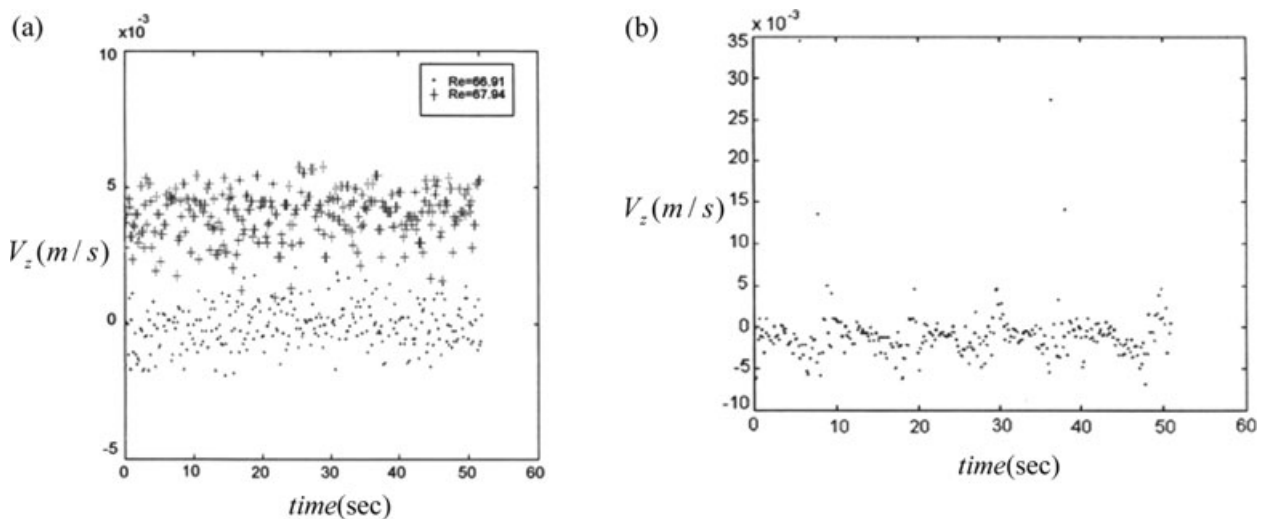


Fig. 3: Speed along the flow axis when the flow becomes unstable: (a) nonmodulated and (b) modulated for Reynolds number = 63.35,  $\varepsilon = 1$ ,  $\omega = 11.778$ , and  $\Omega_2 = 0$

When the fluid is in a one-dimensional stability Couette flow, only radial speed exists. The axial speed measured by LDA is zero. When rotational speed increases and the flow is transformed into a two-dimensional Taylor vortex flow, axial speed appears. Therefore, when the primary measured axial speed in the experiment is not zero, that instant is the stable critical state (Fig. 3).

### MATHEMATICAL BACKGROUND

First, the instability of modulated Couette flow is considered before its transition to modulated Taylor vortex flow. According to the Floquet theorem, the disturbances are expanded by double series with time periodic coefficients,

which have the same period as that of modulation. An algebraic eigenvalue problem is obtained by Galerkin and collocation methods. The QZ algorithm is employed to solve the eigenvalues which determine the stability of flow. The eigenvalue  $\sigma$  is the growth rate of a complex disturbance. The stability of the basic flow can be determined by the real number of the growth rate for a complex disturbance. When  $\sigma_r < 0$ , the entire flow is stable. The disturbance declines as time increases. When  $\sigma_r > 0$ , the disturbance increases over time and the flow becomes unstable. When  $\sigma_r = 0$ , the flow has neutral stability.

Second, the primitive variables of modulated and nonmodulated Taylor vortex flows are solved numerically. The Adam-Bashforth and Crank-Nicolson methods are employed

to discretize the nonlinear and linear terms, respectively, of the Navier-Stokes equations.

For the convenience of problem analysis, we assume that the working fluid is a Newtonian fluid. Except for density all other physical properties are fixed. The change in fluid density satisfies the Boussinesq approximation for gravity and centrifugal force; other items are ignored. The loss of fluid viscosity is also ignored. The dimensionless Navier-Stokes equation and the continuity conditions are then

$$\partial_t \vec{V} + \vec{V} \cdot \nabla \vec{V} = -\nabla p + \Delta \vec{V}, \nabla \cdot \vec{V} = 0 \quad (1)$$

The boundary condition is  $V_r = V_z = 0$ ,  $V_\theta = Re(1 + \varepsilon \cos \omega \tau)$  at  $r = R_1$ , and  $\vec{V} = 0$  at  $r = R_2$ , where  $\vec{V} = (V_r, V_\theta, V_z)$  and the dimensionless factor  $\omega = \omega'(d^2/\nu)$  and  $\tau = t(\nu/d^2)$ ; where  $\nu$  is defined as the kinematic viscosity.

According to Carmi and Tustaniwskyj,<sup>15</sup> flows with axial symmetry become unstable more easily than flows with axial asymmetry. Therefore, this study only considers disturbances of flows with symmetrical state. This flow type can be regarded as a one-dimensional flow with a perturbation and can be expressed as:

$$V_r = 0 + V'_r(r, z, \tau) \quad (2)$$

$$V_\theta = \bar{V}_\theta(r, \tau) + V'_\theta(r, z, \tau) \quad (3)$$

$$V_z = 0 + V'_z(r, z, \tau) \quad (4)$$

$$P = 0 + P'(r, z, \tau) \quad (5)$$

where  $\bar{V}_\theta$  is the basic flow velocity of one-dimensional Couette flow and the perturbations are expressed as:

$$V'_r = \sum_{m=0}^{M-1} \sum_{n=2}^{N+1} A_{mn}(\tau) \phi_n(\xi) \cos m\alpha z \quad (6)$$

$$V'_\theta = \sum_{m=0}^{M-1} \sum_{n=2}^{N+1} B_{mn}(\tau) \phi_n(\xi) \cos m\alpha z \quad (7)$$

$$V'_z = \sum_{m=1}^M \sum_{n=2}^{N+1} C_{mn}(\tau) \phi_n(\xi) \sin m\alpha z \quad (8)$$

$$P' = \sum_{m=0}^{M-1} \sum_{n=0}^{N-1} D_{mn}(\tau) T_n(\xi) \cos m\alpha z \quad (9)$$

Here,  $M$  and  $N$  are the numbers of expanded terms in the Fourier series and Chebyshev polynomials, respectively,  $A_{mn}$ ,  $B_{mn}$ ,  $C_{mn}$ , and  $D_{mn}$  are amplitude coefficients, and  $T_n(\xi)$  is the first type of  $n$ -order Chebyshev polynomials;  $T_n(\xi)$  is defined as follows:

$$T_n(\xi) = \cos(n \cdot \cos^{-1} \xi), \quad n = 0, 1, 2, \dots \quad (10)$$

and  $\xi \in [-1, 1]$ .  $\phi_n$  is the base function that satisfies the boundary conditions and is expressed as:

$$\phi_n = T_n - [1 - (-1)^n] \frac{T_1}{2} - [1 + (-1)^n] \frac{T_0}{2}, \quad n = 2, 3, 4, \dots \quad (11)$$

By analyzing the perturbation into normal modes and utilizing the spectral method<sup>19</sup> to transform the characteristic equation into an algebraic characteristic equation, it can be represented by a matrix.

## RESULTS AND DISCUSSION

Table 2 shows the experimental results and theoretical values. The flow generated an unstable critical value and average experimental value of  $Re_0 = 68.75$ . Compared with the results obtained by other studies, the error rate was  $\pm 1.18\%$ . If the error deviation is added, then the critical value is  $Re_0 = 68.75 \pm 0.81$ . The experimental results acquired by other studies are within the error range. The experimental results are the experimental foundation for the modulated Couette flow. For the measurement of the wave number  $\alpha$ , only a total length of 10 cells in the middle of the flow (equivalent to the total length of five wavelengths) were examined to avoid the influence of the upper and lower boundaries in the experiment. The vortex size was averaged and its wavelength  $\lambda$  was calculated. The precision of this measurement was within 0.1 mm. The wavelength was then calculated by  $\lambda = 2\pi/\alpha$ . Table 2 also shows the average wave number, which is  $\alpha = 3.19$ . The theoretical value calculated for unlimited length was  $\alpha = 3.17$  at the same radius ratio  $\eta = 0.4833$ . The deviation between the experimental result and theoretical value is 0.626%. Additionally, this experiment also examined different aspect ratios, including  $h = 24, 20$ , and 16. The experimental result did not change noticeably, and the critical Reynolds number was within  $Re_0 = 68.75 \pm 0.81$ . Therefore, the aspect ratio does not have a significant effect on the flow stability; this is the same experimental result obtained by Cole.<sup>20</sup>

Under a modulated effect, the inner cylinder rotates with  $\Omega_1 = \bar{\Omega}_1(1 + \varepsilon_1 \cos \omega \tau)$ , radius ratio of  $\eta = 0.4833$ , and  $\varepsilon_1 = 1$ . The stability of the modulated Couette flow is primarily affected by the modulated amplitude and frequency. To compare the modulated effect with the nonmodulated effect, the change rate for the critical Reynolds number is defined here as  $\Delta = (Re_c - Re_0)/Re_0$  (the subscripts are defined as  $c$  being the modulated state and 0 being the nonmodulated state), where  $\Delta > 0$  represent the modulation that has stabilized.

The solid line in Fig. 4 is the theoretical result. At a low frequency, when  $\Delta < 0$ , the critical Reynolds number is lower than that for a nonmodulated effect. This result demonstrates that the modulated effect has an unstable effect on the flow. In addition, when the frequency continues to decrease,  $\Delta$  approached the quasi-steady limit  $-\varepsilon/(1 + \varepsilon)$ . At medium to high frequencies  $\Delta$  increased as frequency increased. Generally, in this frequency range, the modulated effect destabilizes the flow. As frequency decreases, destabilization

**Table 2—Comparison of results from this study and other scholars for nonmodulated Couette flow**

AUTHOR	STUDY METHOD	ASPECT RATIO	RADIUS RATIO	CRITICAL VALUE		WAVE NUMBER	
		$h$	$\eta$	$Re_0$	ERROR RATE %	$\alpha$	ERROR RATE %
Results from this study	Flow visualization optical method	24	0.4833	68.75	—	3.19	—
Donnelly <sup>3</sup>	Torsion measurement method	4	0.5	68.28	0.68	—	—
Simon and Donnelly <sup>4</sup>	Torsion measurement method	5	0.5	68.23	0.76	—	—
Sparrow et al. <sup>21</sup>	Numerical method	Infinite	0.5	68.19	0.81	3.16	0.94
Results from this study	Numerical method	Infinite	0.5	68.186	0.82	3.16	0.94
	Numerical method	Infinite	0.4833	67.94	1.18	3.17	0.626

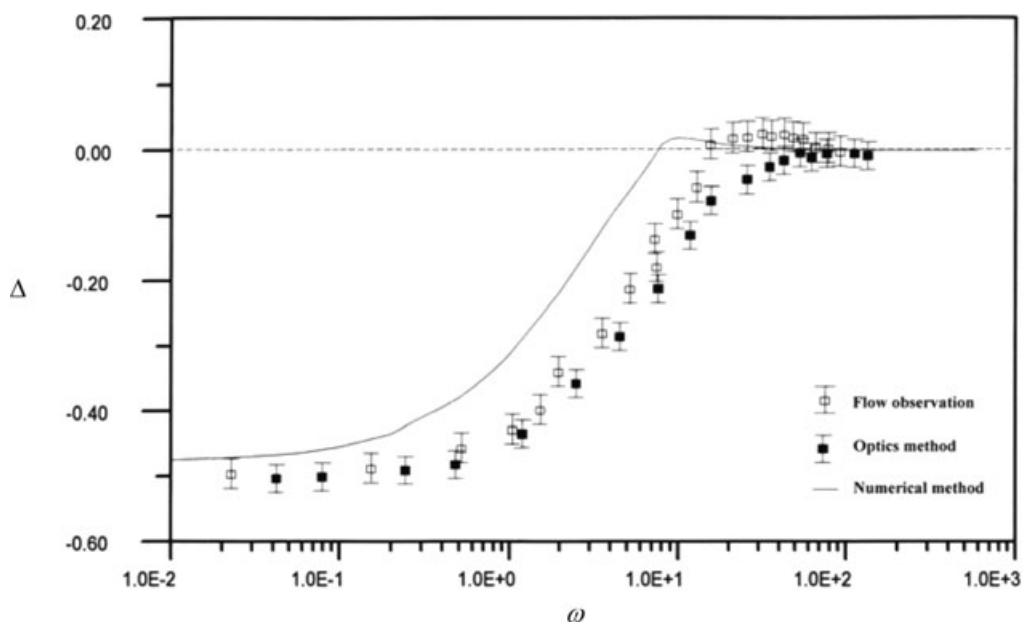


**Fig. 4: Relationship of the relative variable  $\Delta$  versus the modulated frequency shown for the modulated amplitude  $\varepsilon = 1$**

increases. The error for the results in this experiment and the theoretical value was relatively large at medium frequencies. At a high frequency,  $\Delta$  approaches but remains slightly lower than 0. At that point, the modulated frequency slightly destabilizes the flow.

Figure 5 shows the relationship between the relative variable  $\Delta$  of Reynolds number and the amplitude under different frequencies. The dotted line in Fig. 5a is the quasi-steady limit  $-\varepsilon/(1 + \varepsilon)$  when  $\omega \rightarrow 0$ . At an extra low frequency, if the amplitude is high, destabilization is also high. When frequency is  $\omega = 0.063$ , the amplitude increases from 0 to 1.0, and the variable  $\Delta$  of the Reynolds number gradually decreases to around  $-0.5$ . In addition, based on the graph, the experimental result and quasi-steady limit  $-\varepsilon/(1 + \varepsilon)$  are extremely close. When the modulated frequencies are  $\omega = 0.628$  and  $\omega = 6.28$  (Fig. 5b and c, respectively), the relative variable  $\Delta$  of the Reynolds number decreases as the modulated amplitude increases. When the modulated

amplitude is high, the relative variable  $\Delta$  of the Reynolds number decreases and the flow becomes increasingly unstable. However, the degree of instability is lower than that at a low frequency. At a high frequency (Fig. 5d), when the modulated frequency is  $\omega = 62.8$ , the different modulated amplitudes do not have a significant effect on the relative variable  $\Delta$  of the Reynolds number. The modulated amplitude does not significantly influence flow stability.

When the flow is harmonic, the obtained frequency is the same as the frequency during modulated rotation. The speed obtained from the experiment was analyzed with FFT (Fig. 6). With the modulated frequency  $\omega$  in the flow, an emergency was produced at  $\omega/2$ . This energy was higher than the energy in  $\omega$ . This indicates that the flow is a base frequency  $\omega/2$  periodic flow; that is, the subharmonic flow of the modulated frequency. This experimental result is close to the theoretical value, and the trend is the same as that obtained by Youd et al.<sup>16,22</sup>

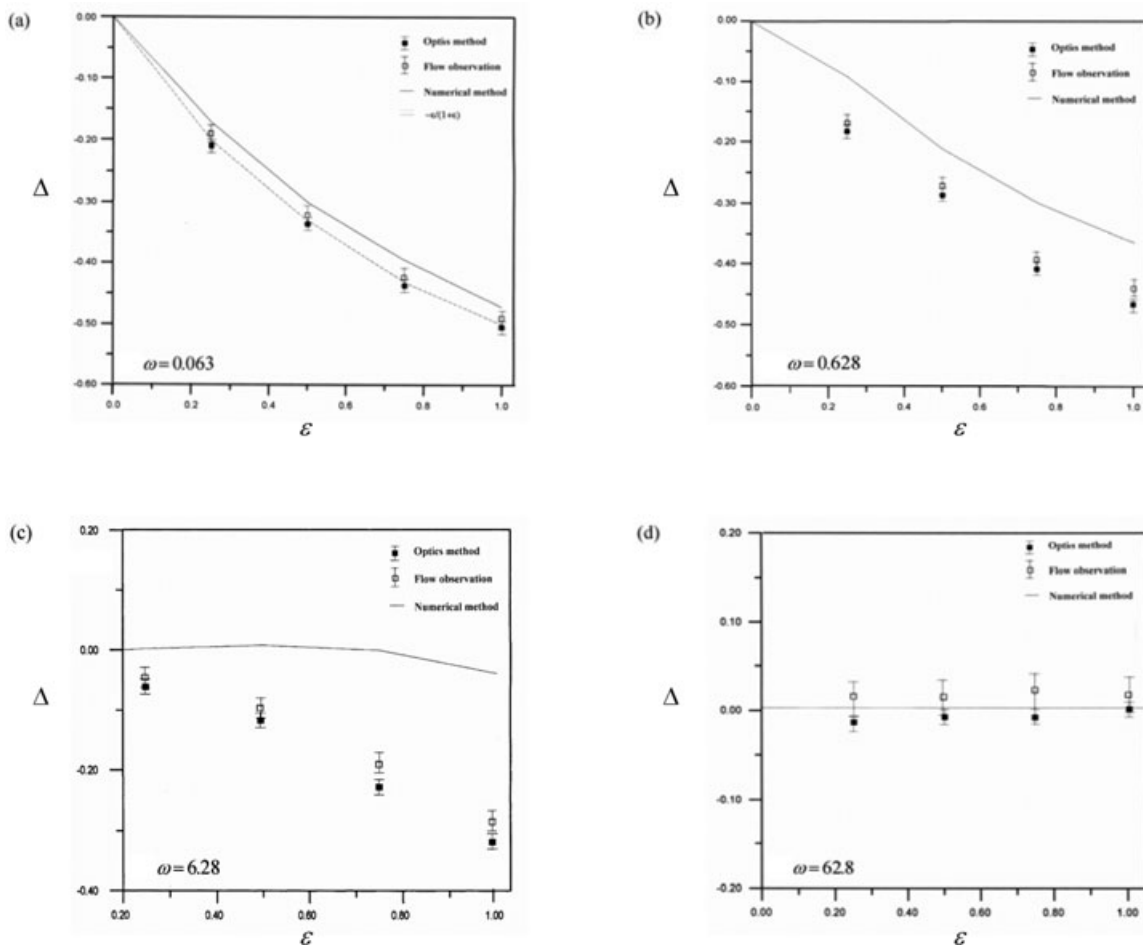


Fig. 5: Relationship between the relative variable  $\Delta$  of the Reynolds number and modulated amplitude  $\varepsilon$  for different modulated frequencies;  $\eta = 0.4833$  and  $h \cong 24$

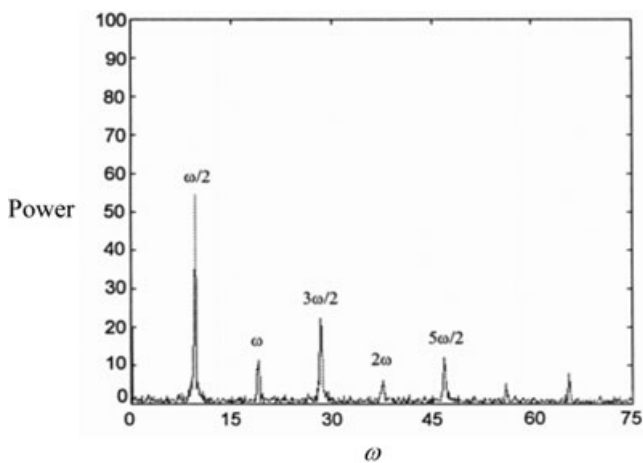


Fig. 6: Spectrum analysis of the subharmonic flow with  $\Omega_1 = \bar{\Omega}_1(1 + \varepsilon \cos \omega \tau)$ ,  $\Omega_2 = 0$ ,  $\eta = 0.4833$ ,  $\varepsilon = 2$ , and  $\omega = 18.75$

## CONCLUSION

We have shown that modulation destabilizes the flow in most frequency ranges. At high frequencies, the critical Reynolds number approaches the nonmodulated critical value  $Re_0$  but will remain slightly lower. At medium-high frequencies, the critical Reynolds number varies with frequency rapidly. At low frequencies, the critical Reynolds number is only slightly affected by the frequency. Additionally, when the modulation amplitude  $\varepsilon = 2$  and the frequency are high for the inner cylinder, a subharmonic flow appears. The aim for future work is now to build on the firm foundation and to utilize the information gained in this study and by other researchers to investigate the onset of wavy vortex flows with more complicated hydrodynamics and at higher Reynolds numbers.

## References

1. Couette, M., "Etudes Sur Le Frottement Des Liquids," *Annales de chimie et de physique* **6**:433–510 (1890).
2. Taylor, G.I., "Stability of a Viscous Liquid Contained between Two Rotating Cylinders," *Philosophical Transactions of the Royal Society of London* **A233**:289–343 (1923).

3. Donnelly, R.J., "Experiment on the Stability of Viscous Flow between Rotating Cylinders I. Torque Measurement," *Proceedings of the Royal Society of London* **A246**:312–325 (1958).
4. Simon, N.J., and Donnelly, R.J., "An Empirical Torque Relation for Supercritical Flow between Rotating Cylinders," *Journal of Fluid Mechanics* **7**:401–418 (1960).
5. Coles, D., "On the Instability of Taylor Vortices," *Journal of Fluid Mechanics* **31**:17–62 (1965).
6. Schwarz, K.W., Springett, B.E., and Donnelly, R.J., "Modes of Instability in Spiral Flow between Rotating Cylinders," *Journal of Fluid Mechanics* **20**:281–289 (1964).
7. Nissan A.H., Nardacci J.L., and Ho C.Y., "The Onset of Different Modes of Instability for Flow between Rotating Cylinders," *AIChE Journal* **9**:620–624 (1963).
8. Marques, F., and Lope, J.M., "Taylor-Couette Flow with Axial Oscillations of the Inner Cylinder: floquet Analysis of the Basic Flow," *Journal of Fluid Mechanics* **384**:153–175 (1997).
9. Lope, J.M., and Marques, F., "Dynamics of Three-tori in a Periodically Forced Navier-Stokes Flow," *Physical Review Letters* **85**:972–975 (2001).
10. Walsh, T.J., and Donnelly, R.J., "Couette Flow with Periodically Corotated and Counterrotated Cylinders," *Physical Review Letters* **60**:700–703 (1988).
11. Gollub J.P., and Swinney, H.L. "Onset of Turbulent in a Rotating Fluid," *Physical Review Letters* **35**:927–930 (1975).
12. Walden, R.W., and Donnelly, R.J., "Reemergent Order of Chaotic Circular Couette Flow," *Physical Review Letters* **42**:301–304 (1979).
13. Donnelly, R.J., "Experiments on the Stability of Viscous Flow between Rotating Cylinders III. Enhancement of Stability by Modulation," *Proceedings of the Royal Society of London* **A281**:130–139 (1964).
14. Hall, P., "The Stability of Unsteady Cylinder Flows," *Journal of Fluid Mechanics* **67**:29–63 (1975).
15. Carmi, S., and Tustaniwskyj, J.I., "Stability of Modulated Finite-gap Cylindrical Couette Flow: linear Theory," *Journal of Fluid Mechanics* **108**:19–42 (1981).
16. Youd, A.J., Willis, A.P., and Barenghi, C.F. "Reversing and Non-reversing Modulated Taylor-Couette Flow," *Journal of Fluid Mechanics* **487**:367–376 (2003).
17. Walsh T.J., Wagner W.T., and Donnelly R.J., "Stability of Modulated Couette Flow," *Physical Review Letters* **58**:2543–2546 (1987).
18. Ganske, A., Gebhardt, T., and Grossmann, S., "Taylor-Couette Flow with Time Modulated Inner Cylinder Velocity," *Physics Letters: Part A* **192**:74–78 (1994).
19. Canuto, C., Hussaini, M.Y., Quarteroni A., and Zang, T.A., *Spectral Methods in Fluid Dynamics*, Springer-Verlag, New York (1988).
20. Cole, J.A., "Taylor-vortex Instability and Annulus-length Effects," *Journal of Fluid Mechanics* **75**:1–15 (1976).
21. Sparrow, E.M., Munro, W.D., and Jonsson, V.K., "Instability of the Flow Between Rotating Cylinders: the Wide Gap Problem," *Journal of Fluid Mechanics* **20**:35–46 (1974).
22. Youd, A.J., Willis, A.P., and Barenghi, C.F., "Non-Reversing Modulated Taylor-Couette Flows," *Fluid Dynamics Research* **36**:61–73 (2005). ■